In-situ Geotechnical Investigation of a Short Section of the Brazos River Post Hurricane Harvey Using a Portable Free Fall Penetrometer

Reem Jaber¹, Nina Stark, Ph.D., M.ASCE¹, Navid Jafari, Ph.D., M.ASCE², Nadarajah Ravichandran, Ph.D., M.ASCE³

¹Department of Civil and Environmental Engineering, Virginia Tech., 200 Patton Hall, Blacksburg, VA 24061. e-mail: reemj@vt.edu

¹Department of Civil and Environmental Engineering, Virginia Tech., 200 Patton Hall, Blacksburg, VA 24061. e-mail: ninas@vt.edu

²Department of Civil and Environmental Engineering, Louisiana State University, 3212D Patrick F. Taylor Hall, Baton Rouge, LA 70803. e-mail: njafari@lsu.edu

³Department of Civil Engineering, Clemson University, 202 Lowry Hall, Clemson, SC 29634. e-mail: nravic@clemson.edu

ABSTRACT

Hurricane Harvey, a category 4 hurricane on the Saffir-Simpson hurricane wind scale that approached from the Gulf of Mexico, caused severe flooding in Texas and Louisiana. Recorded water levels along the Brazos River exceeded historic high-water levels, and erosion and slope failures of riverbanks were observed in many locations along the river. A near-surface site investigation was conducted in the Brazos River along a short section in Sugarland, Texas post Hurricane Harvey. In-situ tests were conducted using a portable free fall penetrometer and a chirp sonar. Results showed that sediment properties varied between different locations. Weaker sediments underlying a loose top layer were observed at both riverbanks reaching a penetration depth of ~20 cm, whereas stiffer sediments were found at the center of the river with an estimate of maximum quasi-static bearing capacity ranging from 25 to 300 kPa at sediment depths less than 7 cm. Particle size distributions varied as well depending on the location. Results suggest a correlation between sediment strength and backscatter intensity of the chirp sonar. In summary, in-situ geotechnical properties across and along short sections of the Brazos River exhibited a significant variability, likely governed by the local sediment remobilization processes that was reflected in portable free fall penetrometer and chirp sonar measurements of the riverbed surface.

INTRODUCTION

Sediment dynamics and remobilization processes can affect geotechnical site characteristics impacting subaqueous infrastructure design and performance as well as future erodibility (Balachandar and Kells 1997; Albatal et al. 2017). However, identifying site specific correlations between geotechnical parameters of seabed surface sediments, complex hydrodynamic conditions, and geomorphodynamics remains a challenge.

Portable free fall penetrometer (PFFP) represent an economic method to investigate the uppermost layers of subaqueous sediments (Stoll and Akal 1999; Mosher et al. 2007; Stark and

Kopf 2011). They have emerged as a useful tool particularly in areas of difficult access and for the investigation of sediment transport processes (Stark et al. 2014; Albatal and Stark 2016; Albatal et al. 2019). Stark and Kopf (2011) monitored changes of sediment strength with the formation of scour at an offshore wind energy converter, and Albatal et al. (2019) documented the changes in vertical sediment strength profiles with active sediment transport processes in a nearshore environment. Thus, it is envisioned that the PFFP can reveal new information on spatiotemporal variations in sediment strength and stratification from extreme river flooding events and associated riverine geomorphodynamics.

Acoustic methods can serve the assessment of seabed layering and monitoring of the evolution of scour (Govindasamy et al. 2012; Prendergast and Gavin 2014; Saleh and Rabah 2016). For example, chirp sonar is widely used in offshore site investigations to evaluate the stratigraphy of the seabed, often accompanied by core samples and Cone Penetration Testing (CPT). However, acoustic methods can be constrained by the interference of entrained air, high turbulent flows, and strongly variable bed conditions (Prendergast and Gavin 2014). Therefore, acoustic investigations are commonly performed after flow velocities have returned to normal levels. A reduction of flow velocity can lead to scour hole infill, and thus biased measurements of maximum scour depth (Govindasamy et al. 2012). It is hypothesized that a combination of PFFP and chirp sonar may enable the assessment of actual maximum scour hole depth despite scour hole infill by displaying vertical stratification of layers of different geotechnical properties. This would allow the recording of actual maximum scour hole depths post flooding under safe operational conditions. However, combining PFFP and chirp sonar for geotechnical site characterization in riverine environments post flooding has not been tested before in the context of local geomorphodynamics. In this study, PFFP and chirp measurements were performed along two transects in the Brazos River ten months after Harvey caused severe flooding and an initial analysis of the results is presented.

REGIONAL CONTEXT

The Brazos River is one of the longest river (1,352 km) within Texas. Its watershed stretches from New Mexico to the Gulf of Mexico, and it flows towards the Southeast. The study area is located in the lower part of the Brazos River, close to the cities of Sugarland and Richmond in Fort Bend County (Figure 1). Near Richmond, the river width and the water depth are approximately ranging between 50-100 m and 7-9 m, respectively, under no flood conditions (NWIS 2019).

Hurricane Harvey was a category 4 hurricane on the Saffir-Simpson hurricane wind scale that developed over the Gulf of Mexico in August 2017. Heavy rainfall caused severe flooding along the Brazos River. Water levels recorded were up to a meter higher than historic high-water levels, corresponding also to record levels in the discharge rate (Stark et al. 2017). The USGS river gage 08114000 of the Brazos River at Richmond, TX measured maximum water levels of ~ 16.8 m on August 31 (statistic daily mean ~ 7.6 m), which was associated with a discharge of more than 2,830 m³/s (statistic daily mean ~ 43 m³/s) (NWIS 2019). As a result, erosion and slope failures of riverbanks were observed at many locations along the River, including the area of Sugarland, TX

(Figure 2). The Brazos River is considered highly susceptible to major erosion during flooding events (Blake and Zelinsky 2018). In the span of the last 10 years, the riverbanks next to the survey location have eroded up to 44 m (blue arrow in Figure 2 (c)).

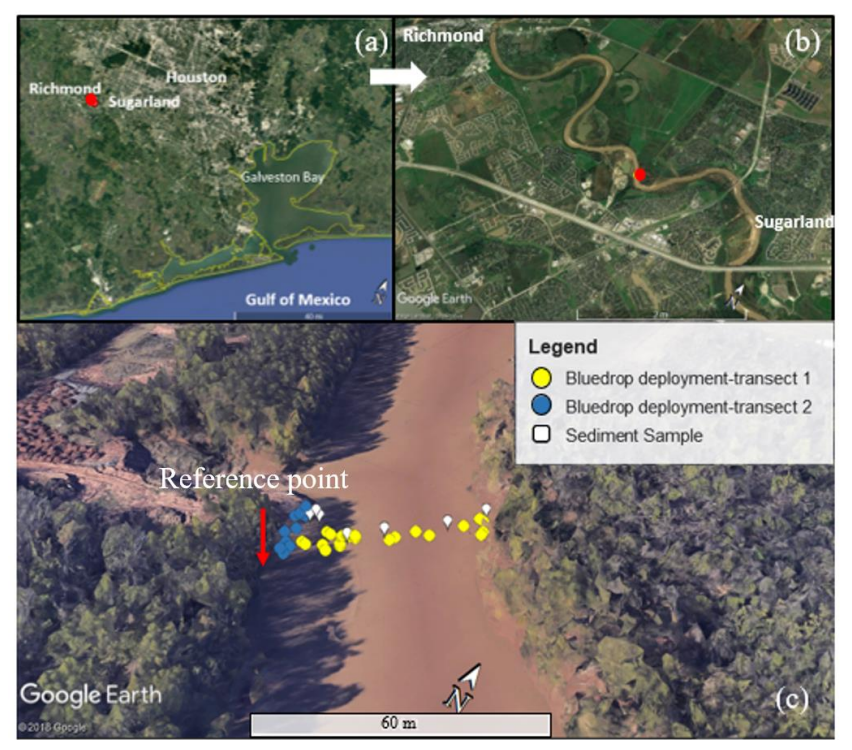


Figure 1. (a) Google earth (2018). Brazos River, Texas. 29°3421.61″ N, 95°41′51.47″ W (b) Zoomed in location of the area (c) PFFP deployment and sediment sampling locations (Map data: Google, SIO, NOAA, U.S Navy, NGA, GEBCO).

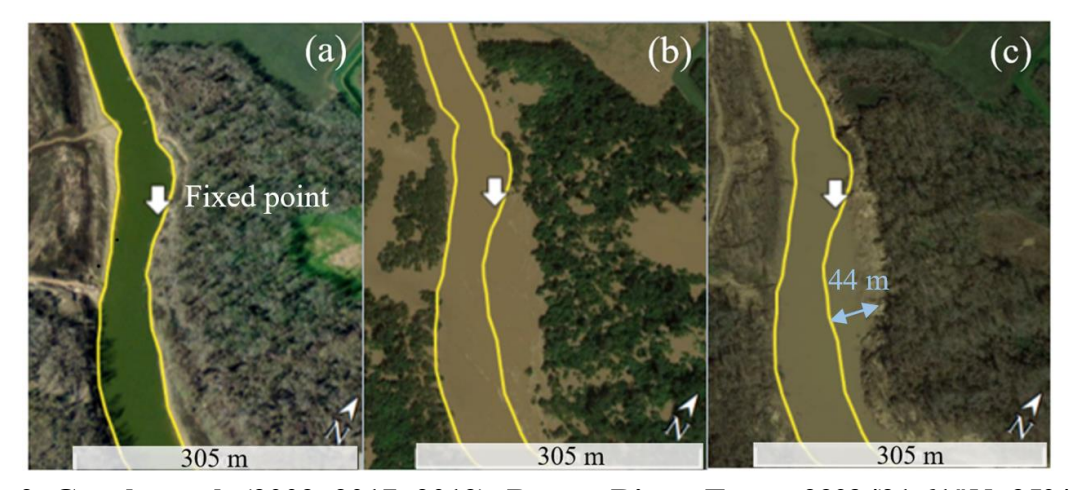


Figure 2. Google earth (2009, 2017, 2019). Brazos River, Texas. 29°3421.61″ N, 95°41′51.47″ W. Changes of shoreline location close to the survey site in: (a) January 2009 (b) August 2017 (c) February 2019. (Map data: Google, SIO, NOAA, U.S Navy, NGA, GEBCO).

METHODS

The PFFP *Bluedrop* has an approximately streamlined shape, weighs 7.7 kg, and measures 63.1 cm in length (Stark et al. 2014). The main body and tail are made of aluminum while the conical tip is made of steel. The device records continuously acceleration/deceleration and pressure at a sampling rate of 2 kHz during free fall through the water column and soil penetration. It is equipped with five vertical accelerometers with capacities of ± 2 g, ± 18 g, ± 50 g, ± 200 g and ± 250 g (with g being the gravitational acceleration) in addition to a dual-axis accelerometer with a capacity of ± 55 g to detect tilt. The pressure transducer measures hydrostatic and pore pressures up to 2 MPa and a resolution of $\pm 4.67 \times 10^{-4}$ kPa.

The device is released under self-weight from a vertical position and falls freely through the water column before it penetrates the riverbed. Upon impact and during advancement through the soil, its deceleration is governed by the soil resistance against the probe. The impact velocity and penetration depth of the penetrometer are derived from the first and second integration of the deceleration-time profile, respectively (Dayal and Allen 1973; Stoll and Akal 1999; Stark and Wever 2009). The derived deceleration-depth profile reflects the sediment type and strength (Dayal and Allen 1973; Stark et al. 2011). Sediment resistance force is assumed as dominant force decelerating the penetrometer and is calculated using Newton's second law and then divided by the area subjected to load to get an estimate of dynamic bearing capacity. Latter is then corrected for strain rate effects and a penetration velocity of 2 cm/s (standard velocity of CPT) based on a strain rate factor correction proposed by Dayal and Allen (1973). This leads to an estimate of an equivalent of cone tip resistance or quasi-static bearing capacity (*qsbc*) (Stark et al 2012; Albatal and Stark 2016).

The PFFP was deployed 35 times in water depths ranging between 1-4 m. Sediment grab samples were retrieved close to PFFP deployments using a ponar sampler (Figure 1). Several attempts were made to retrieve core samples using push tubes, but this remained unsuccessful with the limited equipment available due to loose and soft sediments.

The SyQwest Stratabox HD chirp sonar system is a high-resolution acoustic imaging instrument that can penetrate up to 40 m into the seabed with a vertical resolution up to 6 cm (Stratabox HD manual, 2016). Transmitted sound from the chirp sonar is reflected off seafloor sediment layers that are characterized by different acoustic properties. This allows to measure time and strength of the reflected signal, and based on that, display an image of the riverbed stratigraphy (Stratabox HD manual, 2016). It operates at different frequencies and can be used for marine geophysical surveys of up to 150 m of water depth with a transmit pulse rate from 4 to 10 Hz. It has a blanking distance (i.e., start distance that is affected by proximity to the transducer) of approximately 1 m which can limit measurements in shallow water depths. The PFFP transect across the river was surveyed using the chirp sonar from the western riverbank to the eastern riverbank back and forth (transects 1-a and 1-b, respectively). The chirp sonar results are presented in terms of a normalized backscatter intensity (percentage of the maximum return signal strength). The variations in normalized backscatter intensity are shown at the locations of the deployments, where a higher backscatter intensity means that more of the transmitted acoustic signal is reflected to the receiver (Stratabox HD manual, 2016). A high acoustic reflectivity is often associated with

stiff bottoms and hard objects that prevent further sound propagation into subsequent stratum causing signal reflection and as a result, higher backscatter intensity (Prendergast and Gavin 2014; Stratabox HD manual, 2016).

In this study, deceleration-depth profiles and estimated *qsbc* profiles were utilized to conduct a geotechnical investigation of surficial riverbed sediments at this location post Hurricane Harvey. Preliminary results from the chirp sonar measurements are also presented and discussed in the context of the PFFP results.

RESULTS AND DISCUSSION

Thirty-five PFFP deployments were carried out along two transects: transect 1, across the river and transect 2 along a short section on the western riverbank (Figure 1). The impact velocity of the PFFP ranged between 3.0 and 4.7 m/s with an average of 3.7 m/s and a standard deviation of 0.47 m/s. The maximum decelerations per deployment measured by the penetrometer ranged from 6-42 g, corresponding to maximum qsbc of 6-280 kPa. This is accompanied by an average penetration depth of the PFFP of 5.3 cm along transect 1 and 16.3 cm along transect 2. Significant differences in the vertical deceleration profiles were noted for different locations. The sediments along the western riverbank (transect 2) had low maximum qsbc values ranging between 6 and 20 kPa with an average of 11 kPa and a coefficient of variation (COV) of 41% (Figure 3a). The sediments along transect 1 (cross-river transect) yielded higher maximum qsbc values (Figure 3b), increasing from 25 kPa close to the western riverbank to 285 kPa in the center of the river, and decreasing again to 60 kPa at the eastern riverbank, with a COV of 26% (Fig. 4). The distances across the river were measured with respect to the reference point (red arrow) shown in Figure 1.

A loose sediment top layer (LSTL) defined by low resistance values (i.e., deceleration of PFFP <1g) was observed with varying thicknesses along the two transects; transect 1 and 2 (Figure 4). Figure 3 shows an example of the thickness of the loose layer represented by the blue shading. LSTL thickness varied from 1 to 7 cm for deployments along transect 2 and was negligible (≤ 2 cm) along transect 1 (Figure 4). This layer reflected soft or loose sediments on the top of a stronger substratum and may indicate the presence of a recently deposited or stirred up layer due to localized sediment transport processes (Stark and Kopf 2011; Albatal and Stark 2017). LSTL have been previously reported to be related to remobilization of the top sediment layer under certain hydrodynamic conditions or as a result of a recent deposition of sediment layer (Albatal and Stark 2017; Stark and Kopf 2011).

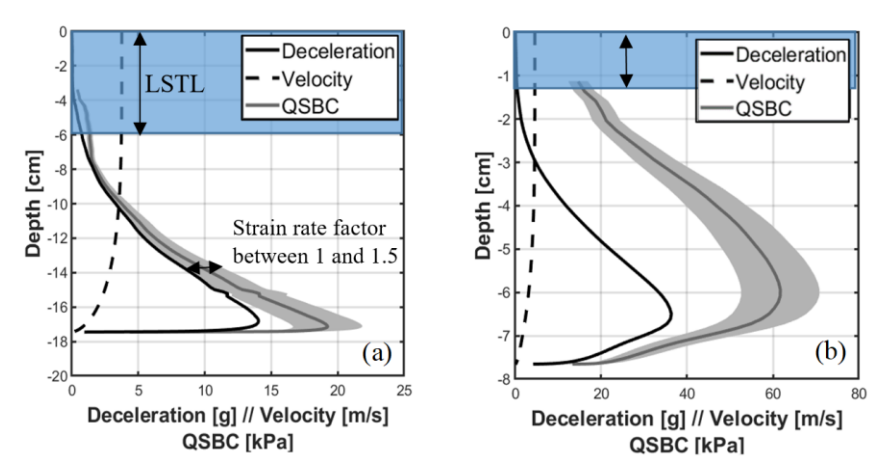


Figure 3. Deceleration, impact velocity, and *qsbc* profiles vs. penetration depth for two deployments of (a) transect 2 (along riverbank) and (b) transect 1 (across the river).

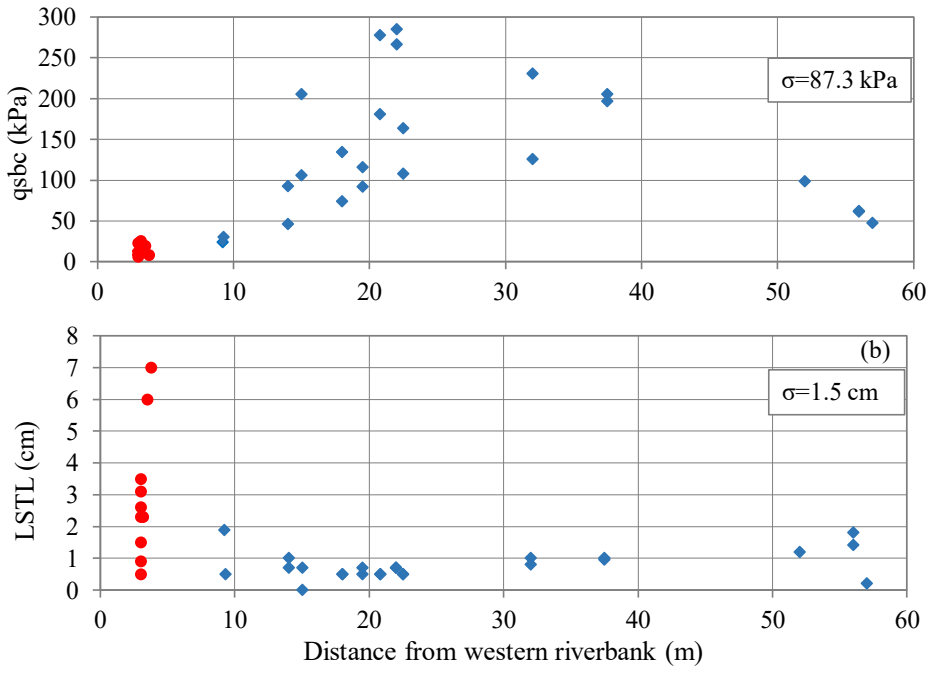


Figure 4. Variation of (a) qsbc and (b) LSTL results for transect 1 (blue color) and transect 2 (red color) at the Brazos River with distance from the western riverbank (σ represents the standard deviation).

Grain size analyses of the samples collected showed that sediments along transect 2 were classified as sands and silty sands according to Unified Soil Classification System (USCS) with fines contents ranging from 0 to 22%, respectively, and an average median grain size (d_{50}) of 0.15 mm, whereas the sediments along transect 1 were classified as poorly graded sands (SP) with 0% fines content and an average d_{50} of 0.27 mm. Thus, higher qsbc results were attributed to sandy sediments across the river with larger d_{50} (Figure 5), which is in line with results by Albatal et al. (2017) that correlate stiffer sediments to larger particle sizes within the range of fine to medium sands. ft³/s

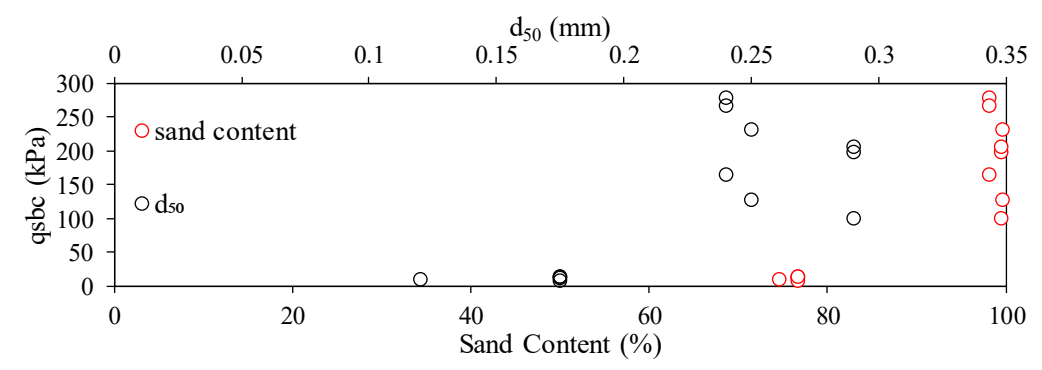


Figure 5. Grain size analysis results (sand content and median grain size d_{50}) of samples.

The pressure transducer in the *Bluedrop* is located at a distance of 7.57 cm from the penetrometer tip. Deployments with a penetration depth of less than 7 cm (70 %) were excluded from the pore pressure analysis due to insufficient penetration depth. However, for deployments with penetration depth >7.57 cm, two types of pore pressure responses were recorded: Types A and B both were characterized by sub-hydrostatic pressures (the measured pressure p < p expected hydrostatic pressure p < p at the early stages of penetration followed by a decrease and increase in pressure respectively after penetration. It should be noted that the recorded pressures should be corrected to account for the Bernoulli effect (i.e., velocity) during free fall. However, this issue remains unaddressed here and the uncorrected values are compared across space and time.

The type A pressure response was only observed along transect 2 (Figure 6), where sediments were classified as silty sand and fine sand. A deviation in the pressure from the hydrostatic line at slightly early stages from the pressure sensors penetration into the soil may be attributed to the pressure wave caused by the high impact velocity of the PFFP, which ejects materials from the impact location as discussed by Lucking et al. (2017). The continuous subhydrostatic response as the pressure sensors penetrate the silty sands with small grain sizes ($d_{50}\sim0.15$ mm) has been previously reported in the literature by Lucking et al. (2017) and correlated to fine sand sediments. The type B pressure response was also observed along the western riverbank, and featured delayed response likely indicating a saturation issue with the porous filter ring, and therefore will be excluded from further discussion.

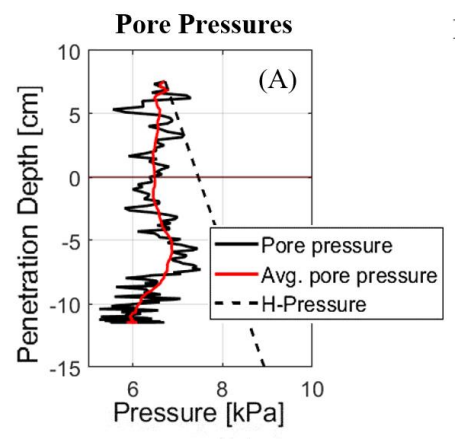


Figure 6. Type A pressure response prior to impact (positive distance) and during penetration (negative distance) of the penetrometer into the riverbed.

Results from the chirp sonar show low backscatter intensities along the riverbanks and high values towards the river center (Figure 7, transects 1-a and 1-b represent chirp transects back and forth, respectively). These findings are in line with the *qsbc* results (Figure 4) confirming the presence of loose mixed sediments along transect 2 and stiff sediments along transect 1. Noise signals in the chirp imagery results indicated the presence of vegetation and debris at multiple locations along transect 1. The high backscatter intensities observed close to the eastern riverbank can be explained due to bottom reverberation effect that occurs in shallow water depths where the sound travels to the bottom and back several times, imitating high backscatter intensities (Stratabox HD manual 2016). Another plausible hypothesis can be related to the chirp location being too close to the riverbank, such that the emitted sound signal was blocked from further penetration due to the riverbank creating a fake impression of a stiff bottom. Such readings leading to 100% normalized backscatter intensity were removed.

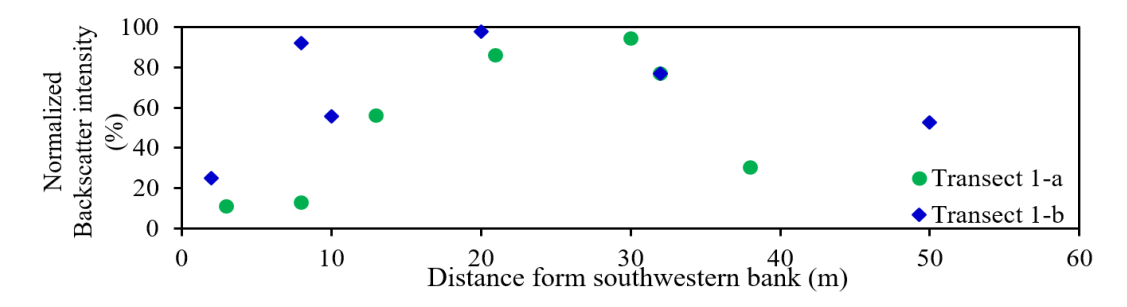


Figure 7. Backscatter intensity results of the chirp sonar along transect 1.

The variation in the sediment strength and pore pressure responses with location were in line with overall trends in soil type and grain size distributions (i.e. finer sediments along transect 2 and coarser sediments along transect 1). The transects studied are located between two river meanders which likely affected local sediment remobilization process due to the erosion and deposition along the outer and inner banks of the meander, respectively (Perucca et al. 2007; Bilici et al. 2018). This would also suggest active sediment transport processes during the flooding events. The variation in the *qsbc* results between the opposite riverbanks is likely due to the higher erosion rate along the eastern riverbank (as shown in Figure 2). The river flow in the southeastern direction facilitated the deposition of sediments at the western riverbank causing the low *qsbc* values and thicker soft top layers. The stiff sediments at the center of the river shown in both the PFFP and the chirp results can be attributed to the decrease in sediment deposition due to the high flow rate at the river center. This is supported by the deceleration and *qsbc*-depth profiles that show no layering for the sediments at this location. In a first attempt, chirp sonar backscatter intensity trends did indeed match the trends in surficial sediment strength measured by the penetrometer (Figures 4 and 7).

CONCLUSION

A reach of the Brazos River bed was investigated post major flooding event in 2017 using a PFFP and a chirp sonar. The aim of the study was to investigate the combined use of PFFP and chirp measurements for local site characterization and investigations of geomorphodynamics. Variations in the quasi static bearing capacity profiles between the two transects were accompanied with variations in the pore pressure response and could be related to differences in grain size distributions. An initial analysis of chirp sonar backscatter intensity of the riverbed surface suggested that changes in sediment strength measured by the penetrometer are reflected in the acoustic backscatter intensity. Thus, the combined use of both instruments to complement each other in future site investigations may reveal more information and fill gaps in understanding of the correlation between geotechnical parameters and local geomorphodynamics in riverine environments. This warrants further investigations of combined use of portable free fall penetrometers and chirp sonar for the investigation of local sediment transport processes and site characterization in riverine environments during normal and extreme river conditions.

ACKNOWLEDGMENTS

The authors acknowledge the National Sciences Foundation through grants CMMI-1822307 and CMMI-1751463 for funding the research presented here. The authors also like to thank particularly Julie Paprocki, Dennis Kiptoo, Mathew Florence, and Brian Harris for their data collection efforts in the field.

REFERENCES

- Albatal, A., Mcninch, J. E., Wadman, H., and Stark, N. (2017). "In-Situ Geotechnical Investigation of Nearshore Sediments with Regard to Cross-Shore Morphodynamics." *Geotechnical Frontiers*, ASCE, 398–408. 10.1061/9780784480472.
- Albatal, A., and Stark, N. (2017). "Rapid Sediment Mapping and In Situ Geotechnical Characterization in Challenging Aquatic Areas." *Limnology and Oceanography: Methods*, 15(8), 690–705. 10.1002/lom3.10192.
- Albatal, A., Wadman, H., Stark, N., Bilici, C., & McNinch, J. (2019). "Investigation of Spatial and Short-term Temporal Nearshore Sandy Sediment Strength Using a Portable Free Fall Penetrometer." *Coastal Engineering*, 143, 21-37. 10.1016/j.coastaleng.2018.10.01.
- ASTM D2487-11. Standard Practice for Classification of Soils for Engineering Purposes (Unified Soil Classification System). *ASTM International*, West Conshohocken, PA.
- Balachandar, R. and Kells J.A. (1997). "Local Channel in Scour in Uniformly Graded Sediments: The Time-Scale Problem." *Canadian Journal of Civil Engineering*, 24(5), 799–807. 10.1139/l97-034.
- Bilici, C., Stark, N., & Hajra, M. G. (2018). "In Situ Geotechnical Characteristics of Surficial Wetland Waterway Sediments." *Journal of Waterway, Port, Coastal, and Ocean Engineering*, 144(6), 04018014.10.1061/ (ASCE) ww.1943-5460.0000462.

- Blake, E.S., and Zelinsky, D.A. (2018). "National Hurricane Center Tropical Cyclone Report Hurricane Harvey". *National Hurricane Center*, National Hurricane Center Tropical Cyclone Report Hurricane Harvey.
- Dayal, U., & Allen, J. H. (1973). "Instrumented Impact Cone Penetrometer." *Canadian Geotechnical Journal*, 10(3), 397-409. 10.1139/t73-034.
- Gavin, k., and Prendergast J. L. (2018). "Reliable Performance Indicators for Bridge Scour Assessments." *TU1406 COST Action*, Barcelona, Spain.
- Govindasamy, A. V., Briaud, J. L., Kim, D., Olivera, F., Gardoni, P., & Delphia, J. (2012). "Observation Method for Estimating Future Scour Depth at Existing Bridges." *Journal of Geotechnical and Geoenvironmental Engineering*, 139(7), 1165-1175. 10.1061/41147(392)4.
- Lucking, G., Stark, N., Lippmann, T., and Smyth, S. (2017). "Variability of In Situ Sediment Strength and Pore Pressure Behavior of Tidal Estuary Surface Sediments." *Geo-Marine Letters*, 37(5), 441-456. 10.1007/s00367-017-0494-6.
- Mosher, D.C., Christian, H., Cunningham, D., MacKillop, K., Furlong, A., and Jarrett, K. (2007). "The Harpoon Free Fall Cone Penetrometer for Rapid Offshore Geotechnical Assessment." 6th International Conference on Offshore Site Investigation and Geotechnic, Society for Underwater Technologies, London, UK.
- NWIS (National Water Information System) (2019). "USGS Current Conditions for the Nation-Station 08114000." < https://nwis.waterdata.usgs.gov/nwis/uv?> (June 10, 2019).
- Perucca, E., C. Camporeale, and L. Ridolfi (2007). "Significance of the riparian vegetation dynamics on meandering rivermorphodynamics." *Water Resour. Res.*, 43, W03430, doi:10.1029/2006WR005234.
- Saleh, M., & Rabah, M. (2016). "Seabed sub-bottom sediment classification using parametric sub-bottom profiler." *NRIAG Journal of Astronomy and Geophysics*, 5(1), 87–95. doi: 10.1016/j.nrjag.2016.01.004
- Stark, N., and Wever, T.F. (2009). "Unraveling Subtle Details of Expendable Bottom Penetrometer (XBP) Deceleration Profiles". *Geo-Marine Letters*, 29(1), 39–45. 10.1007/s00367-008-0119-1.
- Stark, N., and Kopf, A. (2011). "Detection and Quantification of Sediment Remobilization Processes Using a Dynamic Penetrometer." *IEEE/MTS Oceans 2011*, Waikoloa, HI.
- Stark N., Staelens P., Hay AE, Hatcher B., Kopf A. (2014). "Geotechnical Investigation of Coastal Areas with Difficult Access Using Portable Free-Fall Penetrometers." CPT'14.
- Stark et al. (2017). "The Geotechnical Aspects of Coastal Impacts during Hurricane Harvey." (April 5, 2019).">http://www.geerassociation.org/index.php/component/geer_reports/?view=geerreports&layout=build&id=81> (April 5, 2019).
- Stegmann, S., Villinger, H., and Kopf, A. (2006). "Design of a Modular, Marine Free-Fall Cone Penetrometer." *Sea Technology*, (2), 27–33.
- Stoll, R. D., and Akal, T. (1999). "XBP Tool for Rapid Assessment of Seabed Sediment Properties." *Sea Technology*, 40(2), 47–51.
- SyQwest (2016). "StrataBox HD Chirp Operations and Maintenance Manual." http://www.syqwestinc.com/products/sub-bottom-profilers/stratabox (June 5, 2019).